Journal of ELECTRONIC MATERIALS, Vol. 48, No. 9, 2019
https://doi.org/10.1007/s11664-019-07392-3

Thermoelectric Generator for Utilizing Cold Energy of Cryogen Liquids

YURIY LOBUNETS[1,2,3]

1.—Solid Cell Inc., 771 Elmgrove Rd, Rochester, NY 14624, USA. 2.—The Gas Institute of the National Academy of Sciences of Ukraine, 39 Degtyarivska St., 03113 Kiev, Ukraine. 3.—e-mail: yuriy.lobunets@solidcell.com

In this paper, the results of experimental studies of a prototype cryogenic thermoelectric generator (TEG) using transit heat flows in a liquefied natural gas (LNG) evaporator are considered. The main objective was to develop a TEG with low capital cost, integrated directly into an LNG vaporizer, capable of generating electricity at a reasonable levelized cost (LCOE). A demonstration prototype of TEG was created with a power output of 800 W. The prototype used liquid nitrogen (LN_2) instead of LNG as the working fluid. Achieved technical parameters of TEG provide the LCOE decrease to a level of ≈ 0.015 \$/kWh. Such results are achieved using standard components (thermoelectric modules, heat exchangers, etc.) thanks to the optimization of the TEG design.

Key words: Thermoelectric, TEG, specific power of TEG, LCOE, LNG, cold energy, cryogen TEG

List of Symbols

I	Electrical current (A)
J	Dimensionless current density
e	Seebeck coefficient (V/K)
E	Electromotive force (V)
λ	Thermal conductivity (W/cm-K)
σ	Electrical conductivity $(\Omega\ \mathrm{cm})^{-1}$
h	Thermocouple leg length (cm)
n	Number of thermoelectric elements or modules
N	Electrical power (W)
s	Thermoelectric leg cross sectional area (cm^2)
T_o	Determining temperature (K)
T_h	Hot junction temperature (K)
T_c	Cold junction temperature (K)
ΔT	Junction temperature difference (K)
t_h	Heat carrier temperature (K)
t_c	Coolant temperature (K)
Δt	Temperature difference of heat carriers (K)
$\Theta = T/T_\mathrm{o}$	Dimensionless temperature
$\vartheta = t/T_\mathrm{o}$	Dimensionless temperature of fluid
z	Thermoelectric figure-of-merit (K^{-1})
zT_o	Dimensionless thermoelectric figure-of-merit
Q	Heat power flow (W)
η	Efficiency
η_c	Carnot efficiency
α	Heat transfer coefficient ($\mathrm{W/cm^2\ K}$)
R_α, R_λ	Thermal resistance ($\mathrm{cm^2\ K/W}$)
R	Electrical resistance (Ω)
R_L	Electrical load resistance (Ω)
$m = R_\mathrm{L}/R$	Load factor
LCOE	Levelized cost of electricity (\$/kWh)
Bi	*Biot* criterion
Nu	*Nusselt* criterion
Re	*Reynolds* criterion
Pr	*Prandtl* criterion

(Received April 12, 2019; accepted June 19, 2019; published online July 3, 2019)

INTRODUCTION

Increased use of liquefied natural gas (LNG) is a growing trend in the energy industry. According to the World LNG Report,[1] the capacity for liquefaction of natural gas in 2018 has reached 460 million tons per annum (MTPA). In parallel, the capacity of regasification terminals has reached 851 MTPA and continues to increase. The process of the LNG regasification due to the significant latent heat of LNG (550 kJ/kg) and a large temperature difference between LNG and its heating media (the boiling point of LNG is −162°C) has a great energy potential. The aggregate thermal flow of all LNG vaporizers worldwide is about 100 TWh of heat energy. Conversion of this thermal flow to electricity represents significant economic opportunity and societal value, especially because the source of energy during regasification is usually a truly renewable heat source – seawater or ambient air, resulting in zero greenhouse emission. Existing state-of-the-art technology for utilizing this thermal potential is based on the organic Rankine cycle (ORC), direct expansion cycle, or their combinations,[2–7] which is generally plagued by high capital cost, relatively low reliability, and extensive maintenance requirements. Such shortcomings are absent in thermoelectric electricity generators (TEG), which are ideal for use in the conditions of vaporization of cryogenic liquids because these solid-state semiconductor devices have no moving parts, do not require maintenance, and have a comparable efficiency to ORC in the specific conditions of LNG vaporization. Besides, such a generator is essentially a heat exchanger-vaporizer that can serve as an additional cascade in traditional thermodynamic cycles, which will greatly increase efficiency. Possibilities of TEG application were considered in Refs.[8–15] In 2008 Kambe et al.[8] presented a conceptual design of the TEG integrated with the open-rack-type (ORV) LNG vaporizer. The test rig included the encapsulated Bi_2Te_3 modules 50 × 50 mm dimension. Instead of LNG, liquid nitrogen (LN_2) was used. Each module provides electrical power of about 2.5 W and efficiency $\eta \approx 3.5\%$. The evaluated electricity production cost was 16 ¥/kWh (approximately 0.15 \$/kWh). In 2016 Weng et al.[9] observed the cryogenic-nitrogen waste-cold-recovery system by using thermoelectric power generator. Approximately the same results were obtained and conclusions were drawn regarding the prospects of such a system. The author carried out an analysis of the influence of heat transfer conditions on the efficiency of such systems.[15] The possibilities of significant improvement of TEG characteristics were shown. Next, this paper is devoted to the experimental verification of the proposed concept.

THEORETICAL FOUNDATIONS

The main goal of the work was a radical reduction of levelized cost of electricity (LCOE) of a cryogenic TEG, at least an order of magnitude. That is, in order to achieve the goal, it is necessary to ensure the conditions under which a standard module 50 × 50 mm will power level N ≥ 25 W. First of all, it is necessary to determine the conditions under which the module can achieve such power. In the general case, the power of the module is:

$$N = n\frac{(e\Delta T)^2}{\frac{h}{s\sigma}}\frac{m}{(m+1)^2} = nzT_o\eta_c Q_\lambda\frac{m}{(m+1)^2}, \quad (1)$$

where $\eta_c = \Delta T/T_o$—Carnot efficiency; $Q_\lambda = \lambda s\Delta T/h$—heat flux of heat conductivity.

To determine the temperature mode of the module it is necessary to consider the problem of heat transfer in the system “Energy Source – Thermoelectric module – Heat Sink”. This problem was considered in the author’s previous articles.[15,16] In the general form, it can be represented as a nonlinear system of equations, which includes:

- dimensionless thermal conductivity equation:

$$\frac{\partial^2\Theta}{\partial Y^2} + \frac{J^2}{zT_o} = 0, \quad (2)$$

- dimensionless equation of thermal balance on a hot surface:

$$Bi_h[\vartheta_h - \Theta(1)] + \Theta'(1) - J\Theta(1) = 0, \quad (3)$$

- dimensionless equation of thermal balance on a cold surface:

$$Bi_c[\Theta(0) - \vartheta_c] + \Theta'(0) - J\Theta(0) = 0. \quad (4)$$

The solutions of Eq. 2 have the form:

$$\Theta(Y) = C_1 + C_2Y - \frac{J^2}{2zT_o}Y^2. \quad (5)$$

Substituting (5) into (3, 4), we get the following system of equations for the determination of constants C_1, C_2:

$$C_1(J + Bi_h) - C_2 = Bi_h\vartheta_h; \quad (6)$$

$$C_1(Bi_c - J) + C_2(Bi_c - J + 1) = Bi_c\vartheta_c + \frac{J^2}{zT_o}\left(1 + \frac{Bi_c - J}{2}\right). \quad (7)$$

Solving the model (2–7) allows you to calculate the temperature mode and define all the parameters of the TEG. As the initial data, it is necessary to determine the properties of the thermoelectric material (zT_o) and the heat transfer conditions determined by the initial temperatures of heat carriers t_{ho}, t_{co}, and the Bi_h and Bi_c criteria. As the model material selected a well known thermoelectric material based on Bi_2Te_3 with properties (α,

σ, λ) are described with sufficient accuracy as polynomials of degree 2 (the coefficients are given in Table I):[17]

$$P_x = a_o + a_1 T + a_2 T^2. \tag{8}$$

According to the problem, the temperature of the cold source is equal to the saturation temperature of LN_2 (t_{co} = − 196°C), the temperature of the heating medium is taken t_{ho} = 20°C. As a base, the properties of a standard thermoelectric module of 50 × 50 mm produced by S&PF "Module" were used. The nominal power of such a module, depending on the heat transfer conditions, is illustrated in Fig. 1. As it follows from the given data, under certain conditions the task can be solved. The determinant factor is the ratio of the thermal resistances of the thermal conductivity $R_\lambda = h/\lambda$ and the heat exchange $R_{\alpha c} = 1/\alpha_c$, $R_{\alpha h} = 1/\alpha_h$, and the electrical resistance $R = h/\sigma$. That is, in addition to the transfer coefficients α, σ, λ, the essential parameter is the leg lengths of the thermoelements h. For the standard thermoelectric modules, this parameter lies within h = 0.5–5 mm. The analysis of the influence of this parameter on the characteristics of the module shows that at $\alpha \leq 0.05$ the increase in leg lengths leads to an increase in the working temperature difference and power, but at high intensities of heat exchange, the negative influence of the growth of internal electrical resistance prevails, which leads to a decrease in the useful power.

This conclusion is illustrated in Figs. 1 and 2, which shows the dependancies of the maximum power of module N on leg length of thermoelements h with a heat transfer intensity α = 0.1 … 0.6 W/cm^2 K. As it follows from the given data, in order to achieve the goal, it is necessary to ensure the conditions:

$$h \leq 1\ \text{mm};$$

$$\alpha_{c,h} \geq 0.3\ \text{W/cm}^2\ \text{K}. \tag{9}$$

HEAT TRANSFER CONDITIONS

The heat transfer conditions in the water channel are well defined and stable, in the cryogenic channel, they have essential features. In the water channel, heat transfer is described by the criterion equation:[18]

$$Nu = 0.021 Re^{0.8} Pr_w^{0.43} (Pr_w/Pr)^{0.25}. \tag{10}$$

It follows from (10) that to support the condition $\alpha_h \geq 0.3$ W/cm^2 K in the water channel it is necessary to maintain a turbulent flow regime with $Re > 3500$. The heat exchange conditions for the evaporation of cryogenic liquids are of a rather

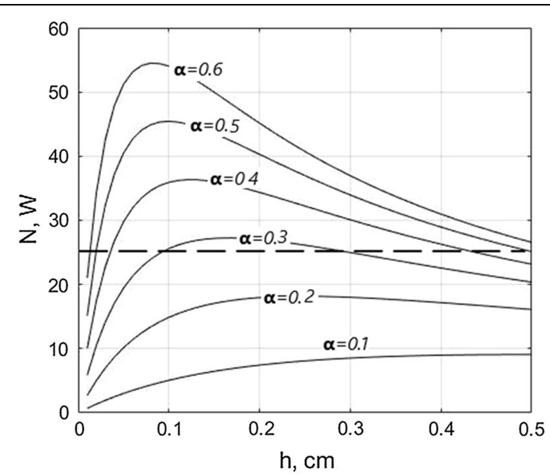

Fig. 1. Influence of h on the max power of module, N.

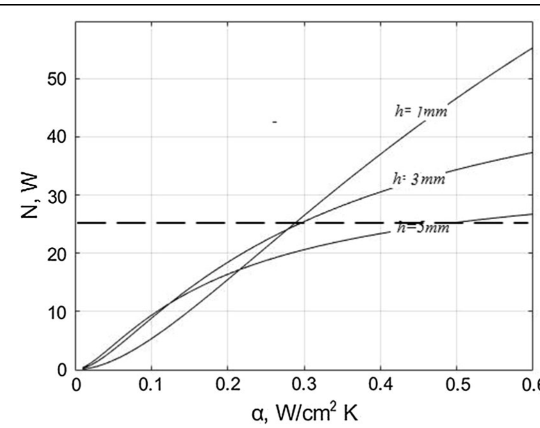

Fig. 2. Influence of α on the max N.

Table I. Polynomial coefficients for the thermoelectric properties

Coefficient	λ_p, W/mK	λ_n, W/mK	e_p, V/K	e_n, V/K	σ_p, $(\Omega m)^{-1}$	σ_n, $(\Omega m)^{-1}$
a_o	3.74236	4.49559	-4.49×10^{-5}	-1.78×10^{-5}	6.40974×10^5	3.6167×10^5
a_1	− 0.01342	− 0.01726	1.28×10^{-6}	1.08×10^{-6}	-2.9551×10^3	-1.4035×10^3
a_2	1.8485×10^{-5}	2.2711×10^{-5}	-1.51×10^{-9}	-1.51×10^{-9}	3.8199	1.68176

complex nature. The liquid passes successively through several phases, each of which is characterized by its flow peculiarities and the intensity of heat exchange. A significant influence on the temperature regime is exerted by the specific density of the heat flux q. As the heat flow q increases, the convective heat transfer passes to the boiling mode (q_o), then the number of evaporation centers on the wall of the heat exchanger increases, and when a certain critical value q_{max} occurs, with the formation of a gas gap between the liquid and the wall, the heat transfer rate decreases sharply and the wall overheating with a jump increases with respect to the liquid temperature. The value of q_{max} depends mainly on the properties and regime of the fluid flow, some influence can also be exerted by the state of the heat exchange surface. The dependence of the superheating of the wall on the heat flux in the region from the boiling point q_o to q_{max} is linear, indicating a constant heat transfer coefficient. After the start of boiling, the amount of the gas phase (the degree of dryness X, %) along the channel increases and at $X \approx 80\%$ the liquid film on the wall dries.[19] It causes the heat exchange rate to drop sharply. Obviously, beyond this boundary, it makes no sense to place the TEG, and the final evaporation and heating of the gas should be carried out in a conventional heat exchanger. Thus, in the working region of interest to us $0 < X < 80\%$, the condition $\alpha_c = const$ can be taken. For LNG, $\alpha_c \approx 0.4–0.7$ W/cm^2 K,[19,20] and for LN_2, which is used as a model fluid, $\alpha_c \approx 0.25–0.6$ W/cm^2 K.[21]

EXPERIMENTAL SETUP OF TEG

The prototype of TEG consists of three rectangular extruded aluminum heat exchangers, designed to introduce the thermoelectric modules between the internal LN_2 channel and external water channels, as shown in Fig. 3. Between heat exchangers two groups of 20 modules of type MT2.6-0.8-263 are clamped (the specification means: 2.6 is the cross-sectional area of the legs, mm^2; 0.8—its height, mm; 263—the number of thermocouples in the module). Liquid nitrogen is fed through the internal heat exchanger with the coefficient of heat transfer

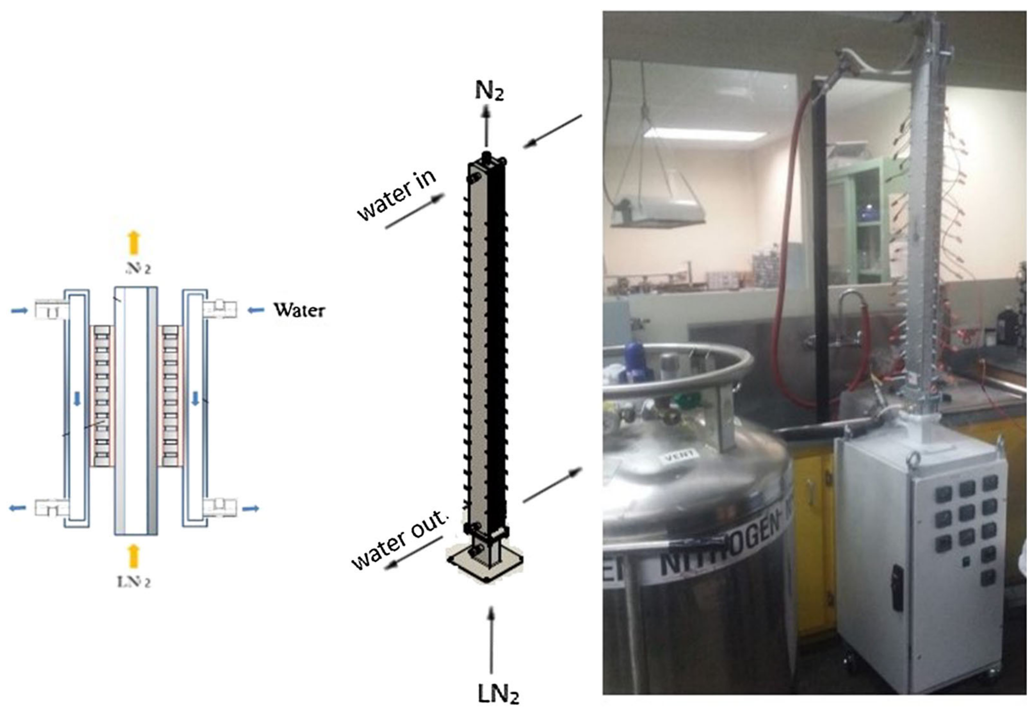

Fig. 3. TEG Prototype circuit and test rig.

Table II. Characteristics of the prototype TEG

Water in t_{in}, °C	Water out t_{out}, °C	Open circuit E_o, V	Short circuit I_o, A	Water flow G, kg/s	Heat flow $Q_o = GC_p(t_{in} - t_{out})$, W	max Power $N_o = E_oI_o/4$, W	Efficiency $\eta = N_o/Q_o$, %
62	51	331	10.2	0.207	9540	844	8.85

$\alpha_c \approx 0.3$ W/cm^2 K. Through external heat exchangers is fed water under the counterflow scheme, with the coefficient of heat transfer $\alpha_h \approx 0.39$ W/cm^2 K. Consequently, the proposed design ensures that the conditions (9) are fulfilled. Under these conditions, the calculated power of the module is $N = 26.8$ Watts (load factor $m = 1.2$). The test rig is equipped with the necessary means of measurement and control.

For purposes of analysis, the temperature distribution of the walls of the heat exchangers, the electromotive force of the TEG and each module, as well as the mass flow rate and temperatures of the heat-carriers were measured.

RESULTS AND DISCUSSION

As an example below the results of measurements of one of the modes of the TEG and their processing (Table II).

The temperature distribution along the walls of heat exchangers is shown in Fig. 4. It is seen that after 2/3 of the length the temperature of the cryogenic channel increases sharply, which indicates a decrease in the intensity of heat transfer in accordance with the transition to a single-phase mechanism, as described above. Accordingly, for a rise in a gap in the power curve of thermoelectric modules—the power decreases from the level of 24–28 W/module to the level of 12–15 W/module (Fig. 5). Such a result is consistent with the previous theoretical analysis.

Thus, the results of the tests confirm the possibility of radically improving the efficiency of the TEG by optimal design and achieving the goal—to increase the specific power TEG by the order of magnitude (from 2.5 W/module up to 25 W/module). At the same time efficiency has almost doubled—from 3.7% to 8.85%. Based on these results one can obtain an estimate of the levelized cost of electricity for a thermoelectric generator that is

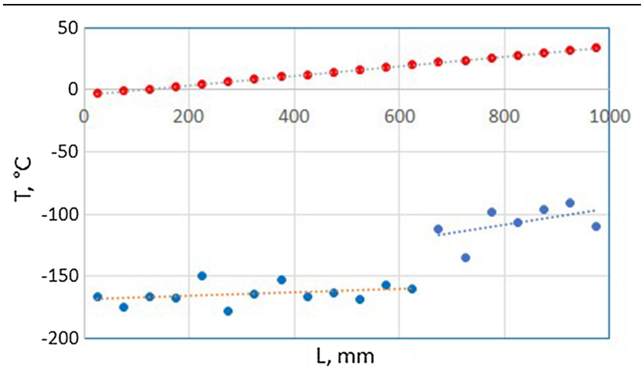

Fig. 4. Temperature distribution of the walls of the heat exchangers.

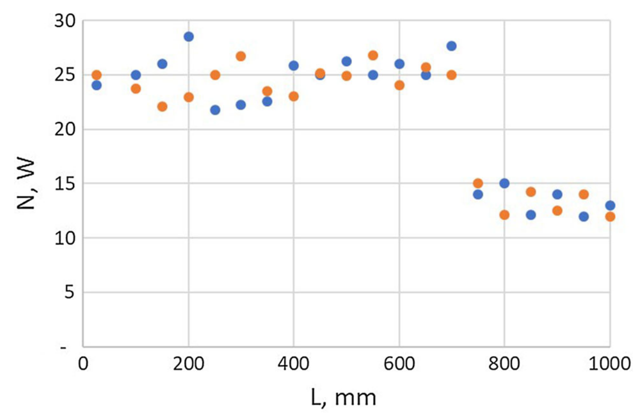

Fig. 5. Module power distribution along the height of the TEG channel.

Fig. 6. Rendering of the 100 kW Cryogen TEG.

used as an evaporator of cryogenic liquids. The LCOE definition formula has the form:

$$\mathrm{LCOE} = (\mathrm{Total Expenses})/(\mathrm{Total Electricity produced})$$

Applying cost estimation model adopted in Ref. 8 and modern prices for TEG components, for the conditions of serial production of TEG with a power of 100 kW, we obtain the following indices:

Design life of the TE modules	10 (years)
Plant availability	80 (%)
Number of TE modules	100 kW/25 W = 4000
Electricity produced in 10 years	100 kW × 10 year × 365 day × 24 h × 0.8 = 7 × 10^6 kWh
TE module cost including mounting and connectors parts	4000 × \$20 = \$80,000
DC/AC inverter and electric distributor	\$100/kW × 100 kW = \$10,000
Heat exchangers	\$50/kW × 100 kW = \$5000
Assembling	\$100/kW × 100 kW = \$10,000
Total Expenses	\$105,000
LCOE	\$105,000/7 × 10^6 kWh = 0.015\$/kWh

Such generator will be looking like a cube measuring approximately 1.5 m (rendering on the Fig. 6).

CONCLUSION

The results of the experimental study of the thermoelectric generator for utilizing cold energy of cryogen liquids are considered. Proposed approaches to designing, which allow to radically increase the power and efficiency of TEG are presented. Due to the optimal design, the specific power increased by an order of magnitude compared with the state-of-the-art TEG of such application, the efficiency has increased almost twice. The use of components produced by the industry has significantly reduced the cost of TEG and provides the competitiveness of electricity—according to preliminary estimates, the LCOE ≈ \$0.015/kWh. Such technical and economic indicators allow us to expect a wide application of TEG in the systems of gasification of liquefied gases, in particular, LNG and LN_2.

ACKNOWLEDGMENTS

This work was supported by the US National Science Foundation under Award Number #1722127, SBIR Phase I: Integrated Thermoelectric Heat Exchanger (iTEG-HX) for Carbon Neutral Electricity Production through Recovery of Cold Energy from Regasification of LNG.

REFERENCES

1. World LNG Report. https://www.igu.org/news/2018-world-lng-report.
2. Cryogenic power generation system recovering LNG's cryogenic energy and generating power for energy and CO_2 emission savings. http://www.osakagas.co.jp/en/rd/technical/1198907_6995.html.
3. Plan for the installation of a Power plant using LNG cold Energy at an LNG terminal. http://members.igu.org/html/wgc2003/.
4. H. Dhameliya and P. Agrawal, *Energy Procedia* 90, 660 (2016).
5. B. Kanbur, L. Xiang, S. Dubey, F. Choo, and F. Duan, *Energy Procedia* 105, 1902 (2017).
6. F. Xue, Y. Chen, Y. Ju, *Energy* 10(3), 363 (2016). https://doi.org/10.1007/s11708-016-0397-7.
7. M. Astolfia, A. Fantolini, G. Valenti, S. De Rinaldis, L. Inglese, and E. Macchi, *Energy Procedia* 129, 42 (2017).
8. M. Kambe, R. Morita, K. Omoto, Y. Koji, T. Yoshida, and K. Noishiki, *Power Energy Syst.* 2, 1304 (2008).
9. E. Jeong, *Cryogenics* 88, 29 (2017).
10. C.-C. Weng, M.-C. Lin, and M.-J. Huang, *Energy* 103, 385 (2016).
11. W. Sun, P. Hu, Z. Chen, and L. Jia, *Energy Convers. Manag.* 46, 789 (2005).
12. Y. Zhao, S. Wang, and Y. Li, *Energy Procedia* 105, 1932 (2017).
13. S. Sivapurapu, *Preliminary Design of a Cryogenic Thermoelectric Generator* (Denton: Univ. of North Texas, 2007).
14. J. Lian, B. Xia, Y.Yin, G. Yang, Y. Yang, X. Gou, E. Wang, L. Liu, J. Wu, in *4th International Conference on Computer, Mechatronics, Control and Electronic Engineering (ICCMCEE 2015)*, 282 (2015).
15. Y. Lobunets, *J. Electron. Mater.* (2019). https://doi.org/10.1007/s11664-019-06943-y.
16. Y.M. Lobunets, *Thermoelectricity* 2, 65 (2014).
17. http://kryothermtec.com/ru/kryotherm-software.html.
18. M. Mikheev, *The Basics of Heat Transfer* (1956).
19. G. Ma, C. Zhang, and L. Zhao, *Adv. Mech. Eng.* 9, 1 (2017).
20. D. Chen and Y. Shi, *Cryogenics* 57, 18 (2013).
21. P. Ardhapurkar, A. Sridharan, and M. Atrey, *Cryogenics* 59, 84 (2014).